Coherent Scatterers at Different Polarizations and Frequencies

Rafael Zandona Schneider, Luca Marotti, Kostantinos P. Papathanassiou
Microwaves and Radar Institute, German Aerospace Center, PO BOX 1116, 82230, Wessling, Germany

Abstract

SAR images of urban areas are characterized by strong geometrical distortions (layover, foreshortening, shadowing) and a high diversity of mainly man-made scattering mechanisms. In order to simplify the analysis of SAR images in urban regions the Coherent Scatterers (CSs) technique has been proposed for the detection of scatterers with point-like behaviour. These deterministic scatterers allow the extraction of information in a simpler and more direct way. In this work, the detection and characterization of CSs at different frequencies and different polarizations is addressed. For that, airborne data acquired at L-, C- and X-band by the E-SAR system of the German Aerospace Center (DLR) over the city of Munich in Germany are used.

1 Introduction

The Coherent Scatterers (CSs) technique for the detection of scatterers with deterministic (i.e., point-like) scattering behaviour in SAR images was proposed in [1], [2]. The detection is performed by correlating SAR images from different looks. In section 2 an overview of the technique is provided.

In [1] and [2] the characterization of CSs concerning their interferometric and polarimetric properties was evaluated. It was shown that they have in general low polarimetric entropy, high amplitude and high interferometric coherence, in agreement to the expected properties of point-like scatterers. The potential of information extraction from CSs as the orientation about the Line of Sight and the dielectric properties of dihedral-like CSs was also addressed.

In [3] a first comparison of CSs at L- and X-band was evaluated for two urban testsites: Dresden and Oberpfaffenhofen, both located in Germany. It was shown that when the images have similar resolution more CSs are detected at L- than at X-band. In this paper the detection and characterization of CSs and their properties at different frequencies (and different polarizations) is further evaluated.

2 Coherent Scatterers Detection

The basic CSs approach [2] evaluates the spectral correlation between two parts of the full image spectrum (two sublooks) to identify deterministic scatterers. Care should be taken if the spectrum of the original image was weighted by a Hamming window in the processing time. In this case, the spectrum should be first divided by the corresponding Hamming function to obtain the original measured image spectrum. The two sublook images are then formed by dividing the total spectrum into two parts (and applying a Hamming window in each one in order to suppress sidelobes), and by shifting them to the same central frequency. The coherence between the two sublook images is estimated and the pixels with high coherence values are interpreted as CSs.

3 The Munich Dataset

In October 2005 SAR data was acquired at L-, C- and X-band over the city of Munich in Germany with the airborne system E-SAR of the German Aerospace Center (DLR). The data at L-band are full polarimetric, at C-band dual polarimetric (HH and HV) and at X-band the channels HH and VV were acquired in repeat-pass mode.

The resolution in range direction of the SLC images at all frequencies is 1.5m and in azimuth is 0.75m at L-band and C-band, and 0.63m at X-band. A resampling in the azimuth direction of the L- and X-band data had to be applied in order to correct for the differences in the images sampling due to different airplane velocities during the acquisition time. Further, a coregistration procedure among all data was necessary.

Fig. 1 shows the Pauli decomposition image at L-band of the Munich city. The azimuth direction is vertical and near range is on the right. On the lower left part of the image the big circular region is the Theresienwiese, where still the temporal structures for the Munich's Oktoberfest were present (the images were acquired one week after the event). Above the Theresienwiese, the Munich central station and part of the rail tracks can be recognized. On the upper right part of the image, the forested region is the Englischer Garten. The Isar river crosses the lower right region of the image.

Note the strong dihedral component (HH-VV) returned from buildings oriented parallel, or almost parallel, to the azimuth flight direction, and that the return from buildings oriented non-parallel to azimuth is dominated by the cross-polarization channel (HV).

Figure 1: Pauli decomposition image. Red: HH-VV, Green: 2HV, Blue: HH+VV. The azimuth direction is vertical and near range is on the right.

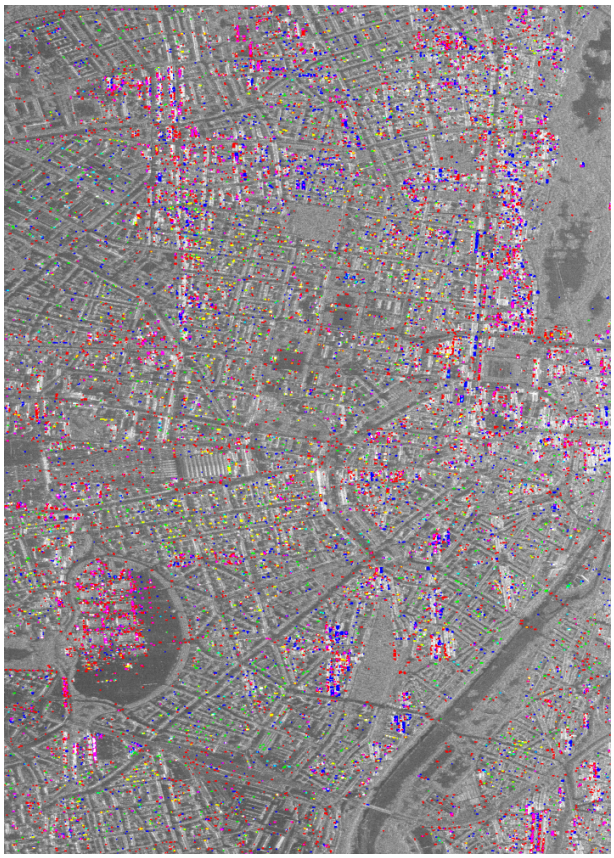

Figure 2: Detected CSs in Pauli basis at L-band. Red: HH-VV, Green: 2HV, Blue: HH+VV.

3.1 CSs at Different Polarizations

Fig. 2 shows the detected CSs at different polarizations (in the Pauli basis) in the L-band data of Munich. A window of 3x7 (range x azimuth) for the estimation of the sublooks coherence and a threshold of 0.98 were applied. HH-VV CSs are presented in red while HH+VV and 2HV CSs are shown in blue and green, respectively.

Note that different CSs are detected at different polarizations. Note also the presence of many dihedral-like CSs (HH-VV). CSs that appear in yellow were detected simultaneously in HH-VV and 2HV. The ones that appear in cyan were detected in HH+VV and 2HV, the ones in pink where detected in HH-VV and HH+VV, and CSs in white were detected in all three Pauli components.

In the park (Englischer Garten) almost no CSs are detected. The density of CSs decreases in areas where the building blocks are strongly oriented (i.e, highly non-parallel) to the azimuth direction, as in the upper left part of the scene. In the dense urbanized areas and in the areas that contain buildings oriented parallel to the azimuth direction, the density of CSs is very high.

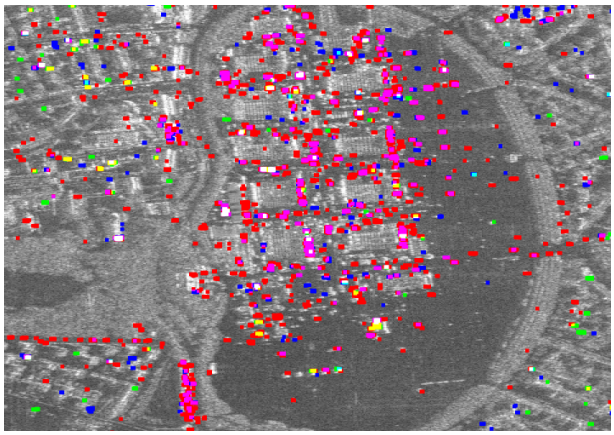

Figure 3: Detail of a subregion of Fig. 2 (Theresienwiese).

Table 1 summarizes the numbers of detected CSs at each polarization channel, together with the common CSs to different channels, for both lexicographic (first line) and Pauli (second line) basis.

Fig. 3 shows an enlargement of the Theresienwiese. Many man-made structures of the Oktoberfest have a deterministic scattering behaviour. Note also the in-line sequence of dihedral CSs in the lower left part of Fig. 3, probably lightpost-to-ground interactions.

3.2 CSs at Different Frequencies

The detection of CSs was performed at L-, C- and X-band using the HH polarization channels and the same window size (3x7) and threshold (0.98) as in the previous section. Fig. 4 shows the CSs at different frequencies in the Munich dataset and Fig. 5 an enlargement of the Theresienwiese. L-band CSs are presented in red while C- and X-band CSs are shown in green and blue, respectively. In this way, scatterers that appear in yellow are common to L- and C-band, in pink are common to L- and X-band, in cyan to C- and X-band and CSs in white are common to all three frequencies.

As in the case of multi-polarization addressed in the previous section, multi-frequency allows the detection of many new CSs, when compared to single frequency. The third line of Table 1 summarizes the numbers of detected CSs at each frequency and in common to different frequencies. As in [3], more CSs were detected at lower than at higher frequencies, although in this case the differences were not very large. Note that the in-line sequence of dihedral CSs in the lower left part of Fig. 3 were detected in all three frequency bands L, C, and X, appearing in white in Fig. 5. This allows us to discuss about the possibility of happening three distinct situations:

1) The resolution cells where CSs were detected at high but not at low frequencies may contain smaller CSs that are not sensed at low but are sensed at high frequencies and have a deterministic scattering behaviour;

2) The resolution cells where CSs were detected at low but not at high frequencies may contain one large deterministic scatterer (that is sensed by all frequencies) but also smaller secondary scatterers that are not sensed at low (due to the longer wavelength) but are sensed at high frequencies (smaller wavelengths are more sensitive to smaller structures). These secondary scatterers introduce phase instability at high frequencies and the resolution cells do not characterize point-like behaviour at high but do characterize at low frequencies;

3) The resolution cells where CSs were detected in common to two or more frequencies may contain deterministic scatterers that are sensed at different frequencies (dihedral, flat plate faced to the radar) and contain no significant secondary scatterers. These scatterers are closest to 'ideal CSs'.

According to this, the physical dimensions of the CSs detected at different frequencies are in general probably different, but not always.

Table 1: Numbers of detected CSs (in thousand) at different polarizations and frequencies. P1: HH+VV, P2: HH-VV, P3: 2HV.

HH	HV	VV	HH∩HV	HH∩VV	HV∩VV	HH∩HV∩VV
135	28.4	83.5	11.3	36.3	7.14	4.79
P1	P2	P3	P1∩P2	P1∩P3	P2∩P3	P1∩P2∩P3
80.1	130	28.4	20.6	4.23	13.0	2.81
L	C	X	L∩C	L∩X	C∩X	L∩C∩X
135	101	95.0	23.5	19.2	30.2	10.8

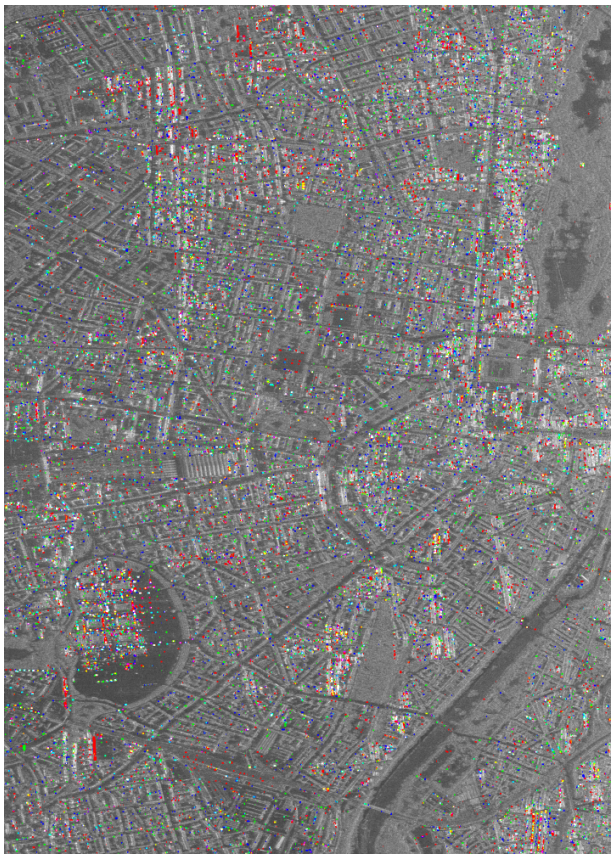

Figure 4: Detected CSs at different frequencies in HH polarization. Red: L-band, Green: C-band, Blue: X-band.

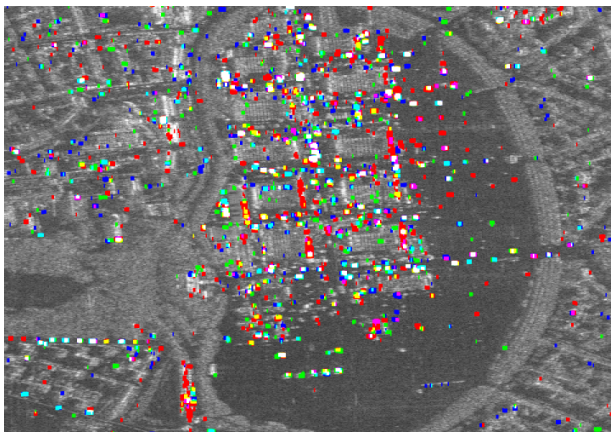

Figure 5: Detail of a subregion of Fig. 4 (Theresienwiese).

4 Characteristics of CSs at Different Polarizations and Frequencies

Fig. 6 shows the histograms of the amplitude at L-band for the whole image, for the CSs detected at L-band, for the common CSs to L- and C-band, for the common to L- and X-band, and for the common CSs to all three frequencies. Fig. 7 shows the corresponding histograms of

the polarimetric entropy while Fig. 8 of the polarimetric alpha angle [4],[5]. The entropy is related to the number of scattering mechanisms present inside the resolution cell while the alpha angle to the type of the dominant scattering mechanism. High entropy values indicate multiple while low entropy only one single scattering process inside the resolution cell. Low values of alpha indicate surface, values around $45°$ indicate dipole, and high values dihedral scattering [4], [5]. The entropy and alpha angles were evaluated using the full-polarimetric L-band data.

One can see that, although not always, CSs have in general much higher amplitude than non-CSs. Furthermore, the common CSs to different frequencies tend to have even higher amplitudes. Similar is the behaviour of the CSs entropy. CSs have in general a lower polarimetric entropy than the rest of the scatterers in the images, as expected, and the CSs detected in common to different frequencies have even lower entropy. Concerning the alpha angle, it can be seen that while the majority of the scatterers in a SAR image of an urban area are dipole-like, the CSs are in their majority dihedral and surface-like scatterers. This behaviour is emphasized for the CSs common to different frequency bands.

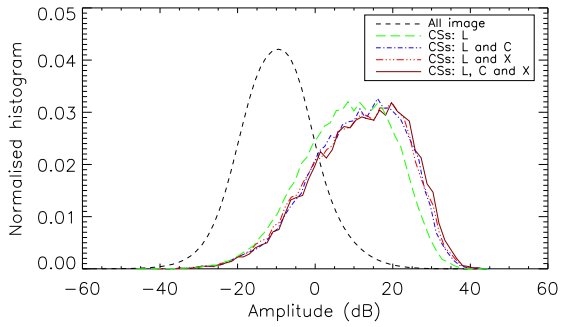

Figure 6: L-band amplitude histograms of the whole image and of CSs detected at different frequencies.

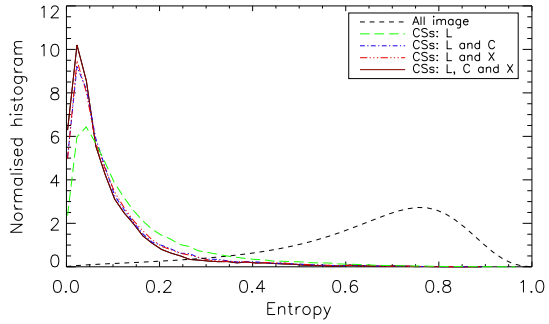

Figure 7: Entropy histograms of the whole image and of CSs detected at different frequencies.

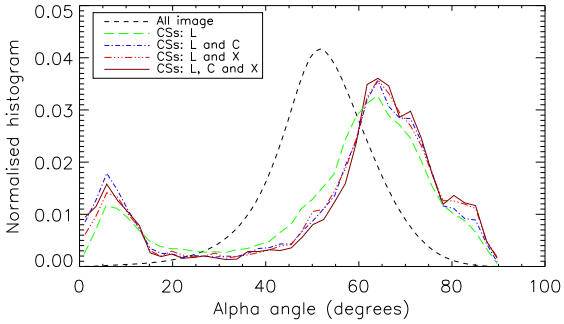

Figure 8: Alpha angle histograms of the whole image and of CSs detected at different frequencies.

5 Conclusions

It was verified that like polarimetric, frequency diversity carry new information concerning scatterers with point-like behaviour in urban areas. The density of detected CSs has been increased by using multi-frequency as well as multi-polarization data. Due to the difference in the wavelengths, the physical dimensions of the CSs detected at different frequencies should be in general different, however not always. The CSs detected in common to different frequencies are scatterers that are closer to ideal point scatterers, with higher amplitude and lower polarimetric entropy. In these cases the responses at each frequency correspond probably to the same physical scatterer inside the resolution cell. Furthermore, the type of the scattering mechanisms dominated by such 'ideal CSs' are mainly dihedral and surface (or flat plates).

References

[1] R. Z. Schneider, K. P. Papathanassiou, I. Hajnsek, A. Moreira: *Analysis of Coherent Scatterers over Urban Areas*, POLinSAR'2005, Frascati, Italy, January 2005.

[2] R. Z. Schneider, K. P. Papathanassiou, I. Hajnsek, A. Moreira: *Polarimetric and Interferometric Characterization of Coherent Scatterers in Urban Areas*, IEEE Trans. Geoscience and Remote Sensing, vol. 44, No. 4, April 2006.

[3] R. Z. Schneider, K. P. Papathanassiou, I. Hajnsek, A. Moreira: *Coherent Scatterers in Urban Areas: Characterisation and Information Extraction*, FRINGE'2005, Frascati, Italy, December 2005.

[4] S. R. Cloude and E. Pottier: *A review of target decomposition theorems in radar polarimetry*, IEEE Trans. Geoscience and Remote Sensing, vol. 34, no. 2, pp. 498-518, March 1996.

[5] S. R. Cloude and E. Pottier: *An Entropy based Classification Scheme for Land Applications of Polarimetric SAR*, IEEE Trans. Geoscience and Remote Sensing, vol. 35, no. 1, pp. 68-78, January 1997.